Analytica Chimica Acta 1032 (2018) 32–39

Contents lists available at ScienceDirect

Analytica Chimica Acta

journal homepage: www.elsevier.com/locate/aca

Multiway analysis through direct excitation-emission matrix imaging

Mirta R. Alcaraz [a, b, c], Ezequiel Morzán [d], Cecilia Sorbello [a, c], Héctor C. Goicoechea [b, c], Roberto Etchenique [a, c, *]

[a] Departamento de Química Inorgánica, Analítica y Química Física, INQUIMAE, Facultad de Ciencias Exactas y Naturales, Universidad de Buenos Aires, Intendente Güiraldes 2160, Ciudad Universitaria, Pabellón 2, Buenos Aires, C1428EGA, Argentina
[b] Laboratorio de Desarrollo Analítico y Quimiometría (LADAQ), Cátedra de Química Analítica I, Facultad de Bioquímica y Ciencias Biológicas, Universidad Nacional del Litoral, Ciudad Universitaria, Santa Fe, S3000ZAA, Argentina
[c] Consejo Nacional de Investigaciones Científicas y Técnicas (CONICET), Godoy Cruz, 2290, Buenos Aires, C1425FQB, Argentina
[d] Comisión Nacional de Energía Atómica, General Paz 1499, Buenos Aires, B1650KNA, Argentina

HIGHLIGHTS

- Inexpensive direct imaging of Excitation-Emission matrix is feasible in video rate.
- Fast data acquisition allows the generation of high-order data that fulfill multi-linearity.
- PARAFAC analysis indicates that bilinear EEM and trilinear LC-EEM data can be successfully generated.

GRAPHICAL ABSTRACT

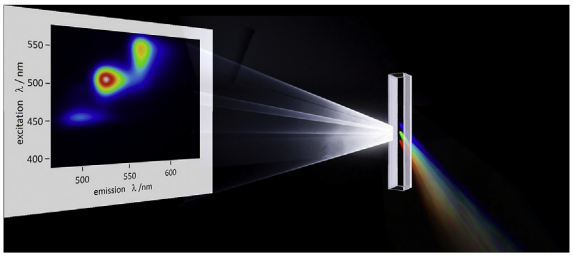

ARTICLE INFO

Article history:
Received 12 April 2018
Received in revised form
21 June 2018
Accepted 25 July 2018
Available online 28 July 2018

Keywords:
Higher-order data analysis
Excitation-emission matrix
Imaging
Chemometrics

ABSTRACT

In this work, a direct in-flow methodology for the acquisition of excitation-emission fluorescence matrices is presented. The system is particularly suited for measurements in the order of tens of milliseconds. A light source operated in continuous mode is dispersed through a grating and focused onto a square-section capillary. Under the spatially resolved excitation, the emission is collected, dispersed through a second grating and further focused onto a CCD array sensor. To allow the wavelength accuracy, a spectral calibration was performed registering the scattering signal of a dispersive element using interference filters ranging from 340 nm to 740 nm. The theoretical performance of the method was analyzed and second-order data obtained for different analyte mixtures are presented and discussed. PARAFAC was applied to evaluate the trilinearity of the obtained data. Mathematical evaluation by means of the criterion of similarity corroborates the agreement between experimental pure spectra and spectral profiles retrieved from PARAFAC. Moreover, the feasibility of the spectrometer to obtain second-order data for analyses with quantitative aims was demonstrated. Finally, fast data acquisition was proved by monitoring a chromatographic analysis of dye mixtures for the generation of third-order LC-EEM data. Here, an improvement in the resolution of the different instrumental modes was demonstrated.

1. Introduction

Among usual analytical techniques, molecular fluorescence spectroscopy is perhaps the most versatile and sensitive approach for the analysis of a wide range of samples. For a single fluorophoric

* Corresponding author. Departamento de Química Inorgánica, Analítica y Química Física, INQUIMAE, CONICET, Facultad de Ciencias Exactas y Naturales, Universidad de Buenos Aires, Intendente Güiraldes 2160, Ciudad Universitaria, Pabellón 2, Buenos Aires, C1428EGA, Argentina.
E-mail address: rober@qi.fcen.uba.ar (R. Etchenique).

https://doi.org/10.1016/j.aca.2018.07.069
0003-2670/

system, conventional steady-state fluorescence measurements offer clean determinations, with very low background contribution and ease of work [1,2]. In last years, unconventional steady-state fluorescence techniques, i.e. synchronous [3], total synchronous [4] and excitation-emission fluorescence matrix spectroscopy [5,6], have become powerful tools for the analysis of multi-fluorophoric systems, either for static or flow-through configuration experiments, such as flow-injection analysis (FIA) [7] or liquid chromatography (LC) [8,9].

One of the main characteristic of molecular fluorescence is that the excitation and emission spectra are broad. This fact implies a drawback in multi-analyte analysis due to the spectral overlap of the different compounds present in the sample. Among the several strategies that have been proposed to overcome these troublesome facts, multivariate calibration has demonstrated to be a good alternative that allows extracting the most relevant information from a system, both with quantitative and qualitative aims [10–12]. In particular, second- and higher-order data analyses have the feature that is a great benefit for the analysts: the so-called "second-order advantage" [13]. Those calibration methods are able to achieve this advantage, which means that they are capable to accurately detect several components even in presence of interferences or unexpected components. This second-order advantage is object of profuse experimental and theoretical research.

In multivariate analysis, it is important to evaluate if the collected data are linearly independent in the different instrumental modes that was registered. Only under this condition the concept of multi-linearity is fulfilled, e.g., bilinearity for second-order data, trilinearity for third-order data, and so on. However, this is a difficult goal to achieve for signals that are changing in time, e.g., flow analysis or chemical kinetics. In this kind of systems, the continuous change in the sample composition during the measurement of the different variables or instrumental dimensions (excitation, emission, residence time, etc.) introduces dependences between the measured parameters and, thus, errors in the determination [14].

It is noteworthy that modern analytical instrumentation facilitates the generation of multi-way data. However, performing time-dependent experiments with higher-order data acquisition is still a challenge for chemometricians and analytical chemists. The main inconvenient relies in the recording rate of the detectors, which is generally slower than the variation rate of the observable measure (e.g., kinetic rate or chromatographic peak elution). In the recent literature is possible to find a wide number of publications reporting analytical methodologies based on the generation of third-order time-dependent data using fluorescence detection [8,15,16]. The authors inform different ways to compensate the lag between rates, either changing the experimental conditions or modifying the instrumental configuration. At present, these alternatives seem to be the most effective strategies to tackle the problem, even though the total time of the analysis or the analytical and chemical performance could be affected.

The obvious solution to the problem of lack of multi-linearity in time-dependent measurements is to perform them faster, in principle, by enhancing the data acquisition rate. For excitation-emission matrix (EEM) generation, the scan rate of the measurement is a tough issue. Using a typical two-monochromator instrument, obtaining a complete EEM may take on the order of minutes, although the most modern fast-scanning fluorescence spectrometers can diminish the recording time on the order of seconds. The inner mechanical movements involved in the wavelength selection of both excitation and emission spectrum registering imply that the speed of the measurements cannot be substantially increased; however, spectrometers having array-based emission detectors can be faster. In this matter, fluorescence microscopy, including two-photon and single-molecule techniques, introduces a whole range of new possibilities, essentially, for fast analysis in micro-sized environments [17].

Myrick et al. [18,19]. have presented a way to perform direct measurements of EEM by bidimensional excitation and emission spatial dispersion. In their system, an ISA/Jobin-Yvon imaging spectrograph was used to direct the vertically dispersed excitation onto a standard cuvette, while the emission light was collected at 90° and directed to a Spex Czerny/Turner device that further horizontally disperses the emission towards a cooled charged coupled device (CCD). In this way, a bidimensional 115×105 field is generated. Following a different strategy, Peng [20], Yuan [21], and Andrews [22] used Fourier or Hadamard transform to elicit a EEM through interferometers or digital encoding. All this methods seem to be reliable, precise and rather fast, although expensive, given the necessity to use commercial spectrometer modules or sophisticated optics to achieve their goals.

In this work, following the path pioneered by Myrick, a simple, very fast, in-flow EEM spectrometer setup is presented. This setup uses rather inexpensive optics accessories and has the characteristic that can be easily upgraded by means of simple modifications. The basic apparatus is described and experimental results for higher-order multivariate analysis are depicted. Additionally, theoretical limits of the approach by using only available optical elements are analyzed.

2. Materials and methods

2.1. Reagents and samples

All the reagents were analytical grade. Tetrasodium fluorescein (Flu), resorufin (Res), 7-hydroxy coumarin (7-OHC), pyranin (Pyr), rhodamine B (RhB), 2,3-dicianohydroquinone (DCHQ) and eosin Y (EoY) dyes were commercially acquired and used as purchased. Anhydrous sodium hydroxide (NaOH, pellets) was purchase from Anedra (La Plata, Argentina). LC grade methanol (MeOH) was acquired from Sintorgan S.A. (Buenos Aires, Argentina).

Stock standard solutions of each dye were prepared by dissolving the proper amount of each drug in water. Concentrations of the stock solutions were in the order of 10^{-6} mol L^{-1}.

A calibration set of 15 mixed samples was prepared by transferring the appropriate aliquots of Flu, Res and 7-OHC stock solutions and 50 μL of 1.0 mol L^{-1} NaOH to 2.00 mL volumetric flasks and completing to the mark with distilled water. The samples detailed in Table 1 were built following a central composite design.

A 5-samples validation set was made following a random design and considering dye levels different than those used in the calibration. Additionally, Pyr, RhB and DCHQ were incorporated as interferences in validation samples. The samples were prepared as mentioned above for the calibration set.

For chromatographic analysis ternary mixture samples was prepared by transferring the proper aliquots of EoY, Flu and Res stock solutions and 50 μL of 1.0 mol L^{-1} NaOH to 2.00 mL volumetric flasks and completing to the mark with distilled water.

2.2. Experimental spectrometer setup for the EEM measurements

The basic EEM spectrometer is depicted in Fig. 1. A 75 W xenon (Xe) lamp, operated in continuous mode, was used as light source and was directed through a 200 μm diameter multimode optical fiber, collimated and then dispersed using a plane transmission diffraction grating. A second lens forms an image onto a vertically placed square glass-capillary (1×1 mm path) through which the sample was flowing. The lateral size of the capillary determined the excitation resolution. To prevent undesired reflections in the

Table 1
Calibration and validation samples.

Sample[a]	Fluorescein (10^{-8} mol L^{-1})	Resorufin (10^{-8} mol L^{-1})	7-OHC (10^{-7} mol L^{-1})	Pyranin (10^{-7} mol L^{-1})	RhodB (10^{-8} mol L^{-1})	DCHQ (10^{-7} mol L^{-1})
Cal_01	3.9	8.4	12.4	–	–	–
Cal_02	3.9	8.4	35.6	–	–	–
Cal_03	3.9	24.6	12.4	–	–	–
Cal_04	3.9	24.6	35.6	–	–	–
Cal_05	11.3	8.4	12.1	–	–	–
Cal_06	11.3	8.4	35.6	–	–	–
Cal_07	11.3	24.6	12.4	–	–	–
Cal_08	11.3	24.6	35.6	–	–	–
Cal_09	1.4	16.9	24	–	–	–
Cal_10	14.0	16.9	24	–	–	–
Cal_11	7.6	3.0	24	–	–	–
Cal_12	7.6	30.0	24	–	–	–
Cal_13	7.6	16.9	4.4	–	–	–
Cal_14	7.6	16.9	43.6	–	–	–
Cal_15	7.6	16.9	24	–	–	–
Val_01	2.3	28.0	9.8	27.8	27.8	36.1
Val_02	4.6	6.0	38.7	16.7	22.2	33.7
Val_03	11.6	20	26.1	5.6	44.4	24.1
Val_04	4.6	8.0	26.1	27.8	43.4	43.4
Val_05	2.3	6.0	9.8	16.7	48.2	48.2

[a] Cal_# and Val_# are the calibration and validation samples, respectively.

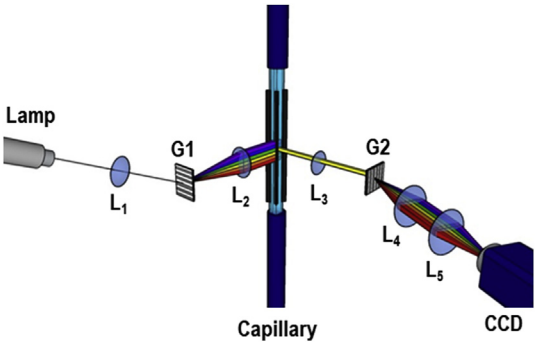

Fig. 1. Scheme of the experimental spectrometer setup for the fluorescence matrix acquisition. L1, L2, L3, L4 and L5 indicate the lenses; G1 and G2 represent the diffraction gratings used in the entrance and the exit of the incident light to the square glass-capillary, respectively.

external faces of the capillary, this was equipped with four black thin layers made with a low reflective black material that were attached to each of the edges. The emission signal of the sample was then collected at 90° with a third lens and horizontally re-dispersed to decompose the emission at each excitation height with a second diffraction grating. Two last lenses focused the complete EEM onto a CCD camera (Point Grey, Flea 2, FL2-03S2M-C) which was directly read by a computer via Firewire interface. The spectrometer was placed on an optical breadboard and was controlled by FlyCapture 2 Viewer.

Wavelength calibration was performed by means of scattering measurements. For this purpose, a μm-size dispersive element was placed into the capillary and interference filters ranging from 340 nm to 740 nm (FWHM = 10 nm) were placed at the light entrance of the instrument. The centroids of the obtained images were determined and the calibration points of both excitation and emission wavelengths were obtained.

All the measurements were done at room temperature.

2.3. Chromatographic measurements

The experiments were performed on a custom-made chromatographic setup equipped with an isocratic pump with manual injection system. The separation was performed at room temperature on a 5 μm SupelcolsilTM LC-18 analytical column (150 × 4.6 mm) (Sigma-Aldrich Inc., Steinheim, Germany) in isocratic mode at 1.0 mL min^{-1} flow rate. The mobile phase consisted in a mixture of MeOH and H_2O in a proportion of 40:60 v/v. The chromatographic setup was hyphenated to the spectrometer setup allowing the on-line EEM registering.

2.4. Data generation and data analysis

The EEM were recorded as. TIFF images using FlyCapture 2 Viewer and further analyzed with ImageJ software, which can be downloaded from https://imagej.nih.gov/ij/download.html, or converted to a double-precision data matrix by using the MatLab function *im2double*.

Data processing and analysis were performed in MatLab (2015b) [23]. PARAFAC modeling was implemented by using the N-way toolbox for MatLab that are available online at http://www.models.life.ku.dk/nwaytoolbox/.

To quantitatively evaluate the comparability of the spectral profiles ($\mathbf{s}_2$) obtained after chemometric decomposition and the real pure spectra of each compound ($\mathbf{s}_1$), the criterion of similarity was employed by using the following expression [24]:

$$s_{12} = \frac{||\mathbf{s}_1^T \mathbf{s}_2||}{||\mathbf{s}_1||\,||\mathbf{s}_2||} \quad (1)$$

The value of s_{12} ranges from 0 to 1, corresponding to no overlapping and complete overlapping between data, respectively.

3. Results and discussion

3.1. General considerations

One of the most important challenges for chemometricians in the analytical chemistry field is the generation of multi-way data that fulfill the concept of multi-linearity. Briefly, from the analytical chemistry standpoint, linearity can be explained as the linear relationship between a dependent and an independent variable, e.g., the concentration of a certain analyte and its measured signal. Hence, the concept of multi-linearity can be interpreted as an extension of the linearity, where the linear relationship is given

between multiple independent variables and a dependent one [25]. In the case of second-order data, EEM signal is described by a concentration that follows a linear relationship between both excitation and emission spectra, fulfilling the concept of bilinearity (in absence of inner filter). In this sense, trilinearity, or multilinearity, follows the same principle. Otherwise, lack of multilinearity occurs and chemometric algorithms that are commonly used for data modeling cannot be applied.

Parallel factor analysis (PARAFAC) is an algorithm that relies on the validity of the Beer-Lambert's law of the target compounds of the sample. This algorithm performs a trilinear modeling of a data set through an iterative least-square optimization [26,27]. Thus, only data that fulfill the concept of trilinearity can be properly decomposed by PARAFAC. Moreover, the resolution of a system with low-rank trilinearity, in absence of linear dependency, is often unique and the profiles obtained after decomposition present physically recognizable information. In addition, constraints can be applied to help reach the uniqueness of the solution. Considering all these properties, this algorithm shows to be a good strategy to evaluate deviations from trilinearity [28,29]. Considering a system with known chemical characteristics, e.g., excitation and emission spectra of each pure component, it is possible to conclude about the reliability of the chemometric decomposition and, in consequence, evaluate the performance of the data generation.

In this work, PARAFAC was applied with the aim to evaluate lack of trilinearity of a 3-way array (built with second-order EEM data obtained for a set of samples) and an third-order LC-EEM data (obtained from a chromatographic procedure coupled to excitation-emission fluorescence matrix detection).

3.2. Second-order calibration

To evaluate the capability of the experimental spectrometer in acquiring second-order data, a validation model was constructed and EEM for several samples were obtained. For this purpose, 12-bits images were registered during 2 s at 5 frames per second (fps) and an exposition time of 75 m s for each sample. In this way, 10 images per sample with a 240 × 320 pixels resolution for excitation and emission wavelength dimension, respectively, were acquired. A typical image obtained as result is depicted as a false colour image in Fig. 2. After conversion to numeric format, the matrices were averaged for further analysis. Thus, an EEM for each sample was obtained and a 3-way array was built comprising the data matrices corresponding to the 15 calibration samples and 1 validation sample. In this way, the 3-way object was of dimension 16 × 240 × 320 for the number of samples, the excitation and the emission wavelength modes, respectively.

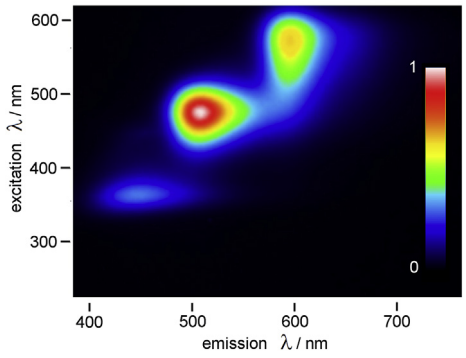

Fig. 2. False colour picture of a raw EEM image corresponding to the Cal_10 calibration sample. Colour scale is given in arbitrary units. (For interpretation of the references to color in this figure legend, the reader is referred to the Web version of this article.)

For the PARAFAC modeling, initial estimates by random initialization were used and non-negativity constraint was applied in the ALS optimization. Core consistency diagnostic analysis (CORCONDIA) [26] was employed to determine the number of spectroscopically active components. Fig. 3 shows the profiles corresponding to the calibrated analytes retrieved from the decomposition of the 3-way data array. For validation samples, 5 factors were necessary to explain the system (explained variance: 99.96%), 3 of which belong to the calibrated compounds and the others to the interferences (Fig. S1, Supplementary Information). As can be seen, excitation and emission spectra of 7-OHC, Flu and Res can be easily identified.

Comparison analysis revealed a good agreement of the PARAFAC spectra profiles with the real spectra of the pure analytes obtained in the same experimental conditions. The s_{12} values obtained by using eq. (1) for excitation/emission spectra of 7-OHC, Flu and Res were 0.99677/0.99644, 0.99639/0.99729 and 0.98907/0.99787, respectively. All this figures indicate a high spectral overlap, which allowed concluding that the retrieved profiles comprise equivalent information as the real pure spectra of each analyte.

Aiming at proving the feasibility of the experimental setup to perform quantitative analyses, a validation study was carried out. For this purpose, the score matrix obtained after PARAFAC decomposition was used since it contains information about the abundance of each individual analyte related to the real concentration of the analyte in the sample. Then, a pseudo-univariate calibration curve was constructed with the information of the calibration samples and concentration predictions both on the calibration and validation samples were computed. The results in terms of the elliptical join confidence region and a comparison between nominal and predicted concentration are depicted in Fig. 4.

As can be shown in Fig. 4a, the elliptical domains obtained for all samples and analytes include the theoretically predicted values for the slope and the intercept, whose are 1 and 0, respectively. On the other hand, Fig. 4 b shows the plot of nominal against predicted values and the corresponding fitting lines for each analyte, whose overlap with the ideal regression line (slope = 1 and intercept = 0). Moreover, the REP % values obtained in the prediction study were 4.9%, 11.2% and 5.2% for 7-OHC, Flu and Res, respectively.

All these observations lead to the conclusion that second-order data are obtained using the spectrometer herein presented, and, then, trilinear arrays are successfully solved by chemometric resolution. Moreover, the feasibility of the spectrometer to obtain second-order data for analyses with quantitative aims was demonstrated. At last, an important aspect needing to be addressed is that considering the fast data acquisition, this procedure can be extended to the generation of higher-order data, e.g., by monitoring kinetics or in-flow through configuration experiments.

3.3. Third-order LC-EEM data analysis

With the purpose of assessing the capability of the experimental spectrometer setup for the monitoring of a chromatographic procedure by generation of third-order LC-EEM data, samples containing 3 well-known analytes were analyzed and PARAFAC algorithm was used.

The experimental configuration used to perform LC-EEM analysis enables to accomplish real-time measurements at multiple wavelengths. In the experiments, 12-bits images were registered whereas the chromatographic procedure was running. The chromatographic run takes a total time of 4.5 min and the EEM images were recorded at 5 fps from the beginning to the end of the analysis with an integrating time of 75 m s. In this manner, during 270 s, 1450 images with a 240 × 320 pixel resolution were acquired. In this way a third-order data array containing 1450 × 240 × 320 data

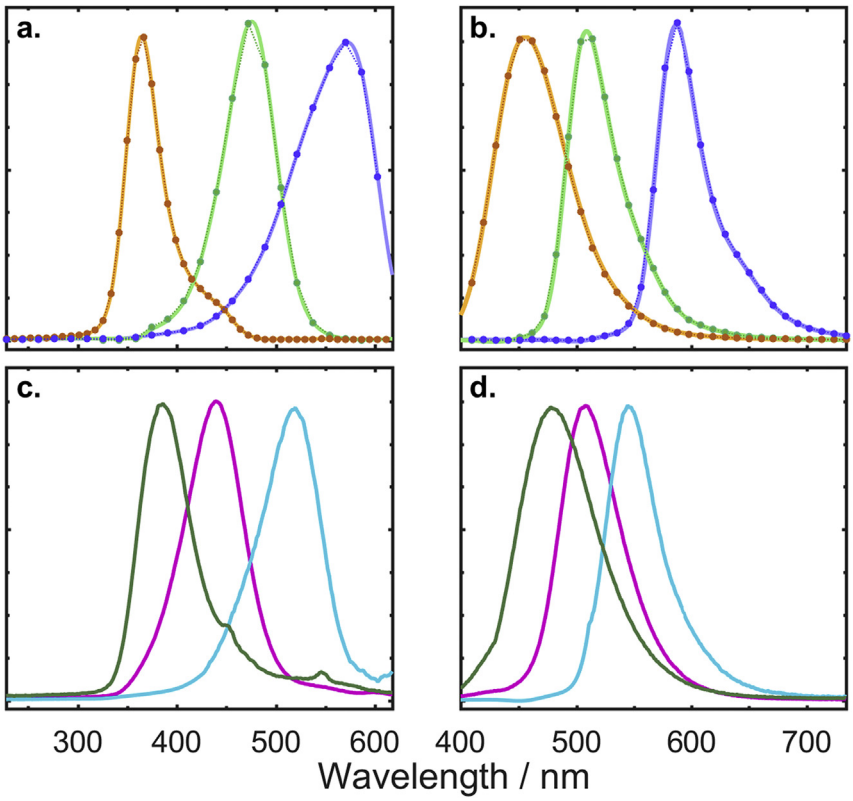

Fig. 3. **(A)** Excitation and **(b)** emission spectral profiles reached from PARAFAC decomposition of a set of EEM data generated with the experimental spectrometer. Orange, green and blue lines represent the spectra of 7-OHC, Flu and Res, respectively. Full circles correspond to the excitation and emission spectra of the pure analytes. **(c)** Excitation and **(d)** emission spectra of DCHQ, Pyr and RhB used as interferences in validation samples. (For interpretation of the references to color in this figure legend, the reader is referred to the Web version of this article.)

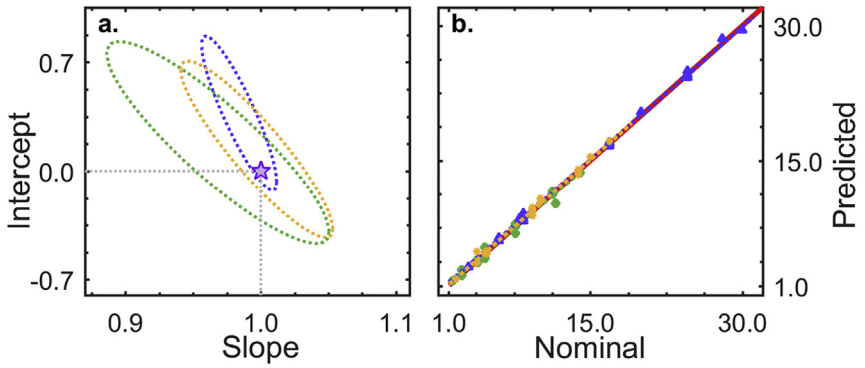

Fig. 4. **(A)** Elliptical joint confidence regions obtained for the prediction results of 7-OHC (orange dashed line), Flu (green dashed line) and Res (blue dashed line) in calibration and validation samples. The pentagram shows the expected value of the intercept (=0) and the slope (=1). **(b)** Nominal against predicted values obtained for calibration and validation samples and the corresponding least-square fitting line for 7-OHC (orange dashed line), Flu (green dashed line) and Res (blue dashed line). Solid red line corresponds to the ideal line with slope = 1 and intercept = 0. (For interpretation of the references to color in this figure legend, the reader is referred to the Web version of this article.)

points for time, excitation and emission wavelength dimension, respectively, was obtained for a given sample. The video of a total chromatographic run can be found as Supplementary Material (videoS5. avi). Here, it becomes necessary to remark that the exposition time used for image acquisition (75 m s) would enable to collect a higher number of images, i.e. allow using a sensor rate higher than 5 fps. However, increasing the number of images for the actual chromatographic procedure would not enhance the resolution of the chromatographic dimension. Additionally, it must be considered that large size data demands superior computational resources and time of analysis. Thus, there is a compromise between the data size and the chromatographic resolution.

To investigate whether the data fulfills the trilinear concept or not, PARAFAC modeling was performed. For the chemometric modeling, initial estimates by random initialization were used and non-negativity constraint in the 3 modes was applied in the ALS optimization. CORCONDIA was employed to determine the number of spectroscopically active components. Fig. 5 depicts the retrieved profiles for a sample containing 3 analytes (For more details see Fig. S2, Supplementary Information).

Supplementary video related to this article can be found at https://doi.org/10.1016/j.aca.2018.07.069.

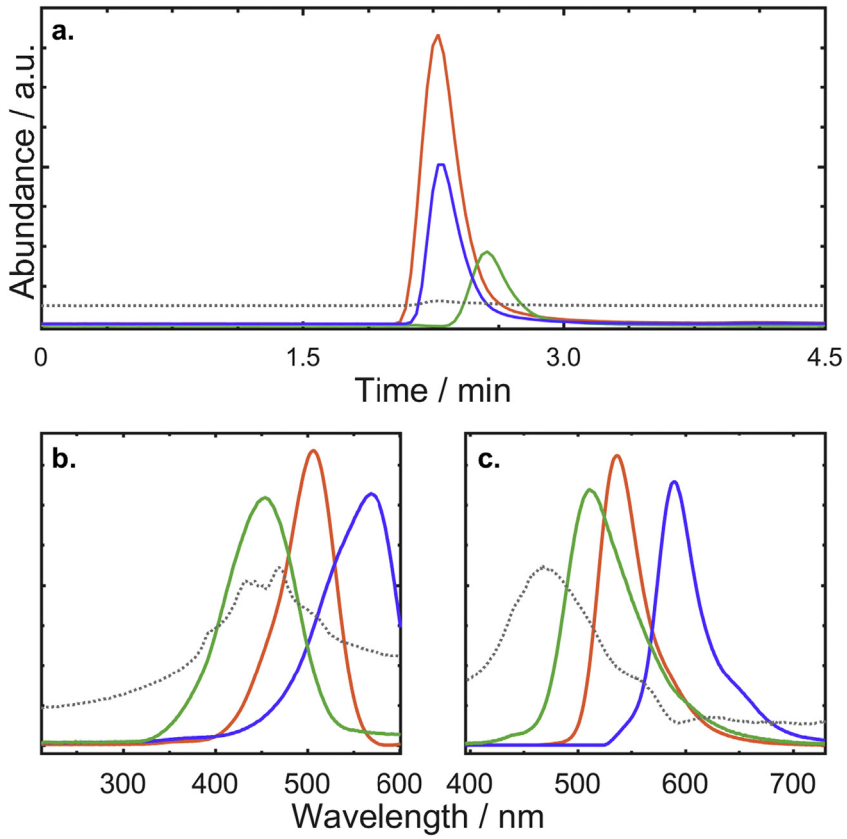

Fig. 5. (A.) Time, (b.) excitation **(c.)** and emission spectral profiles reached from PARAFAC decomposition of the third-order LC-EEM data generated by the experimental chromatographic-spectrometer setup. Green, red and blue lines represent the spectra of Flu, EoY and Res, respectively. Dotted grey lines correspond to the time, excitation and emission spectral profiles of the background. (For interpretation of the references to color in this figure legend, the reader is referred to the Web version of this article.)

As can be seen, 3 resolved profiles were obtained for a sample containing 3 analytes. Fig. 5 shows that the chromatographic peaks and the excitation and emission spectra of each analyte were successfully achieved, even in presence of both strong spectral overlap and high spectra similarity. It is noteworthy that CORCONDIA analysis was in agreement with the real composition of the sample, indicating that 4 factors were necessary to explain the maximum variance of the system, 3 of which belong to the analytes present in the sample and 1 corresponds to the background contribution. The explained variance figure reached after decomposition (97.23%) supports the reliability of the PARAFAC resolution.

Moreover, in order to evaluate the reliability of the obtained results, several samples of same composition were analyzed. In this regards, third-order data were obtained for each sample and trilinearity and quadrilinearity of the generated data were studied. It is important to highlight that in chromatography, time shifts or distortions in the peak shape are usually observed; then, lack of quadrilinearity in 4-way arrays is generally noticed. To overcome this drawback and in an attempt to chemometrically solve a set of third-order data, APARAFAC was applied to an augmented 3-way array.

APARAFAC is an algorithm, which was extensively explained elsewhere [30,31], that allows the decomposition of a set of third-order data that do not fulfill the concept of quadrilinearity. APARAFAC algorithm is based in 3-way PARAFAC modeling and relies in the augmentation philosophy used in MCR-ALS for second-order data analysis. Thereby, APARAFAC is shown as a combination between PARAFAC and MCR-ALS that compiles the individual characteristics of the models. In principle, APARAFAC exploits the ability to bear non-quadrilinear data by means of data augmentation, preserving the original cube structure of the data [29]. For the modeling, third-order data corresponding to the different samples are appending in a way that the trilinearity of the generated augmented object is granted, in this case, an array augmented in the time mode.

APARAFAC results showed that the trilinearity of the data is fulfilled, since the 3 spectral profiles previously achieved for PARAFAC for a given sample (Fig. 4) were successfully retrieved. In Fig. S3, Supplementary Information, lack of reproducibility in retention times between different runs can be observed, demonstrating the lack of quadrilinearity in a 4-way array, and, in consequence, the necessity of using an algorithm that can cope with this phenomenon.

Besides, an important issue to consider when higher-order data are generated is the number of data points in the different instrumental modes. In the present case, third-order array comprised $1450 \times 240 \times 320$ data points for time, excitation and emission wavelength dimension, respectively. The most remarkable issue that can be easily observed is the high resolution obtained in the chromatographic mode, which comprised 1450 points for a chromatographic run of 4.5 min. Moreover, it becomes important to highlight the improvement of the resolution obtained in the 3 instrumental modes in comparison with those reported in the literature for the same kind of data [9,29,30,32,33].

To the best of our knowledge, only 2 works reporting on-line EEM registering of a LC procedure has been published. On one hand, Montemurro et al. [29] report an experimental procedure using a traditional chromatograph and a fast-scanning

spectrofluorimeter in tandem configuration. The authors inform difficulties in the resolution of the generated data, since strong dependence between instrumental modes are observed. Due to the fact EEM are registered in a finite time, the excitation and emission spectra are affected by the concentration distribution of the analyte in the chromatographic analysis. Depending on the registering configuration of the spectrofluorimeter, the spectral modes are affected in different degree. In case emission spectra are taken at different excitation wavelengths, the dependence effect in the acquired spectra will be inconsequential since the spectrum acquisition takes in the order of milliseconds; otherwise, excitation spectra, which is completed in the order of tens of seconds, is strongly dependent of the chromatographic peak feature. Thus, trilinearity of the data is severely lost and no algorithm has been encountered to model this kind of data yet.

On the other hand, to cope with the troubles reported by Montemurro et al. an unconventional experimental chromatographic alternative coupled to a fast-scanning fluorescence spectrometer to perform the same kind of experiments was recently proposed [8]. In that work, the authors found that the mode-dependence effect is diminished when a tube with a larger inner-diameter than those used in conventional chromatographic instruments is connected between the column and the detector. In this way, they informed that variations in the EEM by virtue of the concentration distribution are not observed since a reduction in the linear flow rate of the mobile phase is generated. In these conditions, lack of trilinearity of the obtained data is negligible. However, it is noticeable that even though the undesirable effects by virtue of loss of trilinearity are in principle not observed, there is a remarkable detriment in the chromatographic resolution, obtaining chromatographic peaks with an average time width of ~4 min. At last, despite only 45 chromatographic points were collected for a chromatographic run of 16 min, the results demonstrated the acceptable performance of the chemometric resolution.

Under this scenario and on the basis of obtained results, the presented experimental setup becomes a valuable and powerful alternative to obtain higher-order data that fulfill the concept of multi-linearity. The combination between fast data acquisition with higher-order data analysis is a responsible for the successfully resolution of the system, which its complexity is shown by virtue of strongly spectral overlap in both excitation and emission dimension and the poor chromatographic separation. In presented study, it was demonstrated that resolution for trilinear third-order LC-EEM data enabled the individual identification of highly overlapped signals by analyzing only an individual sample, which represent an important challenge if conventional fluorescence detector is used instead (Fig. S4, Supplementary Information). This fact demonstrates that the use of direct EEM analysis in complex mixtures can be useful even in presence of very poor separative parameters.

It is worth mentioning that this contribution would represent an important step forward for chemometricians and analytical chemists, and it has a potential worth to be explored in other research fields.

3.4. Theoretical limits of the method

In any optical system, for a given overall quality, there is a tradeoff between luminosity and instrumental cost. In this work, aiming to keep the cost of the apparatus as low as possible, the numerical aperture was affected in detriment of sensitivity. However, it is convenient to analyze the performance limits of spatially dispersed direct EEM spectroscopy without considering the cost.

For a 75 W Xe light source (Ocean Optics HPX-2000-HP-DUV), operated in continuous mode, focused onto a multimode 200 μm optical fiber, a typical optical power of about 25 $\mu W\,nm^{-1}$ is expected throughout the majority of the emitted spectra. A concave flat field holographic grating with high numerical aperture (e.g., Horiba 523 00 480) can generate a linear dispersed image of the fiber end directly onto a 200 μm square-section capillary at 30 $nm\,mm^{-1}$. Being the resolving power of the grating much higher than the uncertainty given by the capillary side, a 6 nm resolution in the excitation channel can be obtained. A second (similar) concave grating can be used to achieve the complete 2D matrix, and a 1″ CMOS camera (e.g., BackFly BFS-U3-89S6M-C, Sony IMX255) can be used as sensor. Although this setup becomes several times more expensive than the one presented in this work, the total cost of the setup can be kept below $3000 (American dollars).

In this setup, for a 6 nm resolved band, a 150 μW is expected to be focused onto the capillary, which at $\lambda = 400$ nm would correspond to an excitation of 3×1014 photons s^{-1}. Under these conditions, a very absorptive analyte (Fluorescein, molar extinction coefficient = 92000 $L\,mol^{-1}\,cm^{-1}$) with unity quantum yield of fluorescence needs to be at a concentration of 2×10^{-9} mol L^{-1} to emit 25000 photons s^{-1}. Assuming a 8.8 mm emission image (sensor lower dimension) evenly distributed in 44 zones of 200 μm each and a 6% of overall optical efficiency (two gratings at 25% each) at a maximum sensor rate of 26 fps, an average of 15 photons are directed to each image element. The CMOS sensor presents an absolute sensitivity of 4.83 photons to equal the noise. In this way, the optical limit of detection would be about 20×10^{-9} mol L^{-1}, which corresponds to a concentration of 7 ppt.

4. Conclusions

A simple, inexpensive and robust spectrometer setup was presented for fast excitation-emission fluorescence matrix measurements of samples both in static and in flow-through configuration conditions. The capability of the experimental spectrometer in acquiring second-order data was demonstrated by constructing a validation model with further PARAFAC analysis. Mathematical comparison analysis revealed a good agreement of the PARAFAC spectra profiles with the real spectra of the pure analytes obtained in the same experimental conditions, allowing concluding that the retrieved profiles comprise equivalent information as the real pure spectra of the analytes. The accuracy of the recovery results were proved by applying the elliptical join confidence region test, obtaining elliptical domains that include the theoretically predicted values for the slope and the intercept.

On the other hand, the capability of the experimental setup for the on-line monitoring of a chromatographic procedure by generation of third-order LC-EEM data was also proved. PARAFAC analysis aids to conclude that the third-order data obtained fulfilled the concept of trilinearity, remarking the fact that no data preprocessing was necessary to facilitate the chemometric decomposition. The most noticeable improvement of the present setup is the possibility of obtain data with high resolution both in chromatographic and spectral domains.

It was also detailed that adequate modifications of the setup would lead to important improvements in the detectability and performance of the instrument, at the price of a moderate increment of the total cost.

In the light of the obtained results, the presented experimental setup represents a valuable and powerful tool to obtain multi-linear higher-order data, which is of particular interest for chemometricians and analytical chemists. In addition to the fact that this contribution represents an important step forward for chemometrics, it has a potential worth to be explored in other research fields, essentially, for physicochemical or biological investigations.

Acknowledgments

This research was supported by the National Agency for Science and Technology Promotion, CONICET, and the University of Buenos Aires. H.G and R.E. are staff of CONICET. M.R.A. and C.S gratefully acknowledge the postdoc financial support provided by CONICET.

Appendix A. Supplementary data

Supplementary data related to this article can be found at https://doi.org/10.1016/j.aca.2018.07.069.

References

[1] J.R. Lakowicz, Instrumentation for Fluorescence Spectroscopy, in Principles of Fluorescence Spectroscopy, Springer US, New York, US, 2006, pp. 27–61.
[2] K. Kumar, M. Tarai, A.K. Mishra, Unconventional steady-state fluorescence spectroscopy as an analytical technique for analyses of complex-multifluorophoric mixtures, TrAC, Trends Anal. Chem. 97 (2017) 216–243.
[3] H.T. Temiz, U. Tamer, A. Berkkan, I.H. Boyaci, Synchronous fluorescence spectroscopy for determination of tahini adulteration, Talanta 167 (2017) 557–562.
[4] M. Insausti, A. de Araújo Gomes, J.M. Camiña, M.C. Ugulino de Araújo, B.S. Fernández Band, Fluorescent fingerprints of edible oils and biodiesel by means total synchronous fluorescence and Tucker3 modeling, Spectrochim. Acta a Mol. Biomol. Spectrosc. 175 (2017) 185–190.
[5] C. Cheng, J. Wu, L. You, J. Tang, Y. Chai, B. Liu, M.F.S. Khan, Novel insights into variation of dissolved organic matter during textile wastewater treatment by fluorescence excitation emission matrix, Chem. Eng. J. 335 (2018) 13–21.
[6] W. Mbogning Feudjio, H. Ghalila, M. Nsangou, Y.G. Mbesse Kongbonga, Y. Majdi, Excitation-emission matrix fluorescence coupled to chemometrics for the exploration of essential oils, Talanta 130 (2014) 148–154.
[7] A.P. Pagani, G.A. Ibañez, Four-way calibration applied to the processing of pH-modulated fluorescence excitation-emission matrices. Analysis of fluoroquinolones in the presence of significant spectral overlapping, Microchem. J. 132 (2017) 211–218.
[8] M.D. Carabajal, J.A. Arancibia, G.M. Escandar, On-line generation of third-order liquid chromatography–excitation-emission fluorescence matrix data. Quantitation of heavy-polycyclic aromatic hydrocarbons, J. Chromatogr. A 1527 (2017) 61–69.
[9] M. Montemurro, L. Pinto, G. Véras, A. de Araújo Gomes, M.J. Culzoni, M.C. Ugulino de Araújo, H.C. Goicoechea, Highly sensitive quantitation of pesticides in fruit juice samples by modeling four-way data gathered with high-performance liquid chromatography with fluorescence excitation-emission detection, Talanta 154 (2016) 208–218.
[10] M. Trevisan, R.J. Poppi, Determination of doxorubicin in human plasma by excitation-emission matrix fluorescence and multi-way analysis, Anal. Chim. Acta 493 (2003) 69–81.
[11] S.M. Azcarate, A. de Araújo Gomes, M.R. Alcaráz, M.C. Ugulino de Araújo, J.M. Camiña, H.C. Goicoechea, Modeling excitation-emission fluorescence matrices with pattern recognition algotirhms for classification of Argenine white wines according grape variety, Food Chem. 184 (2015) 214–219.
[12] G.M. Escandar, A.C. Olivieri, N.M. Faber, H.C. Goicoechea, A. Muñoz de la Peña, R.J. Poppi, Second- and third-order multivariate calibration: data, algorithms and applications, TrAC Trends Anal. Chem. (Reference Ed.) 26 (2007) 752–765.
[13] G.M. Escandar, H.C. Goicoechea, A. Muñoz de la Peña, A.C. Olivieri, Second- and higher-order data generation and calibration: a tutorial, Anal. Chim. Acta 806 (2014) 8–26.
[14] A.C. Olivieri, G.M. Escandar, Practical Three-way Calibration, Elsevier, Waltham, USA, 2014.
[15] M. Montemurro, G.G. Siano, M.J. Culzoni, H.C. Goicoechea, Automatic generation of photochemically induced excitation-emission-kinetic four-way data for the highly selective determination of azinphos-methyl in fruit juices, Sensor. Actuator. B Chem. 239 (2017) 397–404.
[16] M.D. Carabajal, J.A. Arancibia, G.M. Escandar, Excitation-emission fluorescence-kinetic data obtained by Fenton degradation. Determination of heavy-polycyclic aromatic hydrocarbons by four-way parallel factor analysis, Talanta 165 (2017) 52–63.
[17] C. Sorbello, R. Etchenique, Intrinsic optical sectioning with upconverting nanoparticles, Chem. Commun. 54 (2018) 1861–1864.
[18] A.R. Muroski, K.S. Booksh, M.L. Myrick, Single-measurement excitation/emission matrix spectrofluorometer for determination of hydrocarbons in ocean water. 1. Instrumentation and background correction, Anal. Chem. 68 (1996) 3534–3538.
[19] K.S. Booksh, A.R. Muroski, M.L. Myrick, Single-measurement excitation/emission matrix spectrofluorometer for determination of hydrocarbons in ocean water. 2. Calibration and quantitation of naphthalene and styrene, Anal. Chem. 68 (1996) 3539–3544.
[20] L. Peng, J.A. Gardecki, B.E. Bouma, G.J. Tearney, Fourier fluorescence spectrometer for excitation emission matrix measurement, Optic Express 16 (2008) 10493–10500.
[21] J. Yuan, L. Peng, B.E. Bouma, G.J. Tearney, Quantitative FRET measurement by high-speed fluorescence excitation and emission spectrometer, Optic Express 18 (2010) 18839–18851.
[22] N.L.P. Andrews, T. Ferguson, A.M.M. Rangaswamy, A.R. Bernicky, N. Henning, A. Dudelzak, O. Reich, J.A. Barnes, H.P. Loock, Hadamard-transform fluorescence excitation-emission-matrix spectroscopy, Anal. Chem. 89 (2017) 8554–8564.
[23] Matlab, MathWorks Inc, Natick, MA, Estados Unidos, 2010.
[24] V. Gómez, M. Miró, M.P. Callao, V. Cerdà, Coupling of sequential injection chromatography with multivariate curve resolution-alternating least-squares for enhancement of peak capacity, Anal. Chem. 79 (2007) 7767–7774.
[25] J.M. Amigo, F. Marini, Chapter 7-Multiway methods, in: M. Federico (Ed.), Data Handling in Science and Technology, Elsevier, 2013, pp. 265–313.
[26] R. Bro, PARAFAC. Tutorial and applications, Chemometr. Intell. Lab. Syst. 38 (1997) 149–171.
[27] R. Boqué Martí, J. Ferré Baldrich, Chapter 1-fundamentals of PARAFAC, in: A. Muñoz de la Peña, H.C. Goicoechea, G.M. Escandar, A.C. Olivieri (Eds.), Data Handling in Science and Technology, Elsevier, 2015, pp. 7–35.
[28] A.C. Olivieri, G.M. Escandar, Chapter 7-parallel factor analysis: nontrilinear data of type 1, in: Practical Three-way Calibration, Elsevier, Boston, 2014, pp. 109–125.
[29] M. Montemurro, G.G. Siano, M.R. Alcaráz, H.C. Goicoechea, Third order chromatographic-excitation–emission fluorescence data: advances, challenges and prospects in analytical applications, TrAC Trends Anal. Chem. (Reference Ed.) 93 (2017) 119–133.
[30] M.R. Alcaráz, S. Bortolato, H.C. Goicoechea, A.C. Olivieri, A new modeling strategy for third-order fast high-performance liquid chromatographic data with fluorescence detection. Quatitation of fluoroquinolones in water samples, Anal. Bioanal. Chem. 407 (2015) 1999–2011.
[31] S.A. Bortolato, V.A. Lozano, A. Muñoz de la Peña, A.C. Olivieri, Novel augmented parallel factor model for four-way calibration of high-performance liquid chromatography–fluorescence excitation–emission data, Chemometr. Intell. Lab. Syst. 141 (2015) 1–11.
[32] M.R. Alcaráz, G.G. Siano, M.J. Culzoni, A. Munoz de la Pena, H.C. Goicoechea, Modeling four and three-way fast high-performance liquid chromatography with fluorescence detection data for quiatitation of fluoroquinolones in water samples, Anal. Chim. Acta 809 (2014) 37–46.
[33] V.A. Lozano, A. Muñoz de la Peña, I. Durán-Merás, A. Espinosa Mansilla, G.M. Escandar, Four-way multivariate calibration using ultra-fast high-performance liquid chromatography with fluorescence excitation–emission detection. Application to the direct analysis of chlorophylls a and b and pheophytins a and b in olive oils, Chemometr. Intell. Lab. Syst. 125 (2013) 121–131.